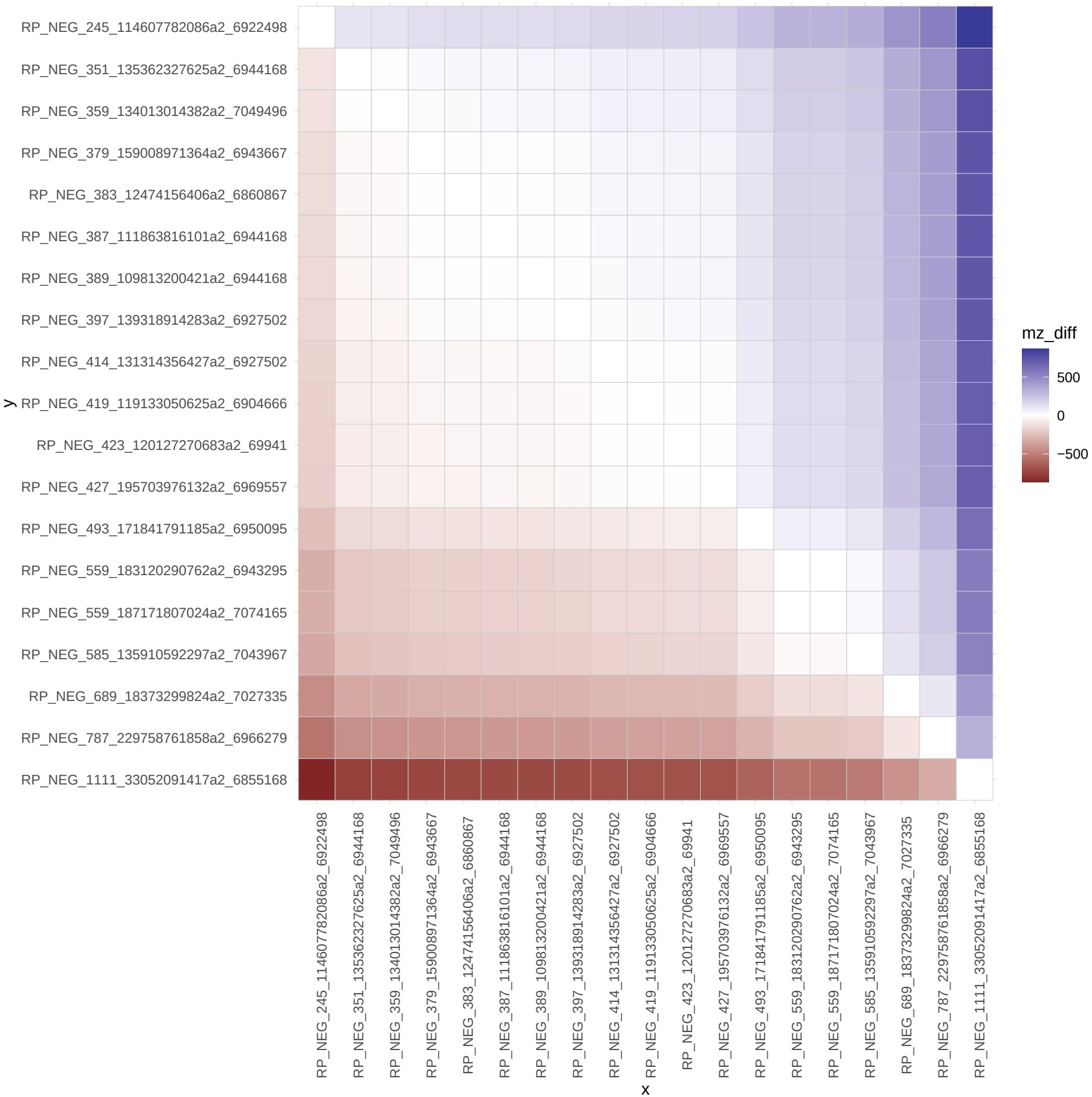
RP_NEG_245_114607782086a2_6922498
RP_NEG_351_135362327625a2_6944168
RP_NEG_359_134013014382a2_7049496
RP_NEG_379_159008971364a2_6943667
RP_NEG_383_12474156406a2_6860867
RP_NEG_387_111863816101a2_6944168
RP_NEG_389_109813200421a2_6944168
RP_NEG_397_139318914283a2_6927502
RP_NEG_414_131314356427a2_6927502
RP_NEG_419_119133050625a2_6904666
RP_NEG_423_120127270683a2_69941
RP_NEG_427_195703976132a2_6969557
RP_NEG_493_171841791185a2_6950095
RP_NEG_559_183120290762a2_6943295
RP_NEG_559_187171807024a2_7074165
RP_NEG_585_135910592297a2_7043967
RP_NEG_689_18373299824a2_7027335
RP_NEG_787_229758761858a2_6966279
RP_NEG_1111_33052091417a2_6855168
y
x
mz_diff
500
0
−500

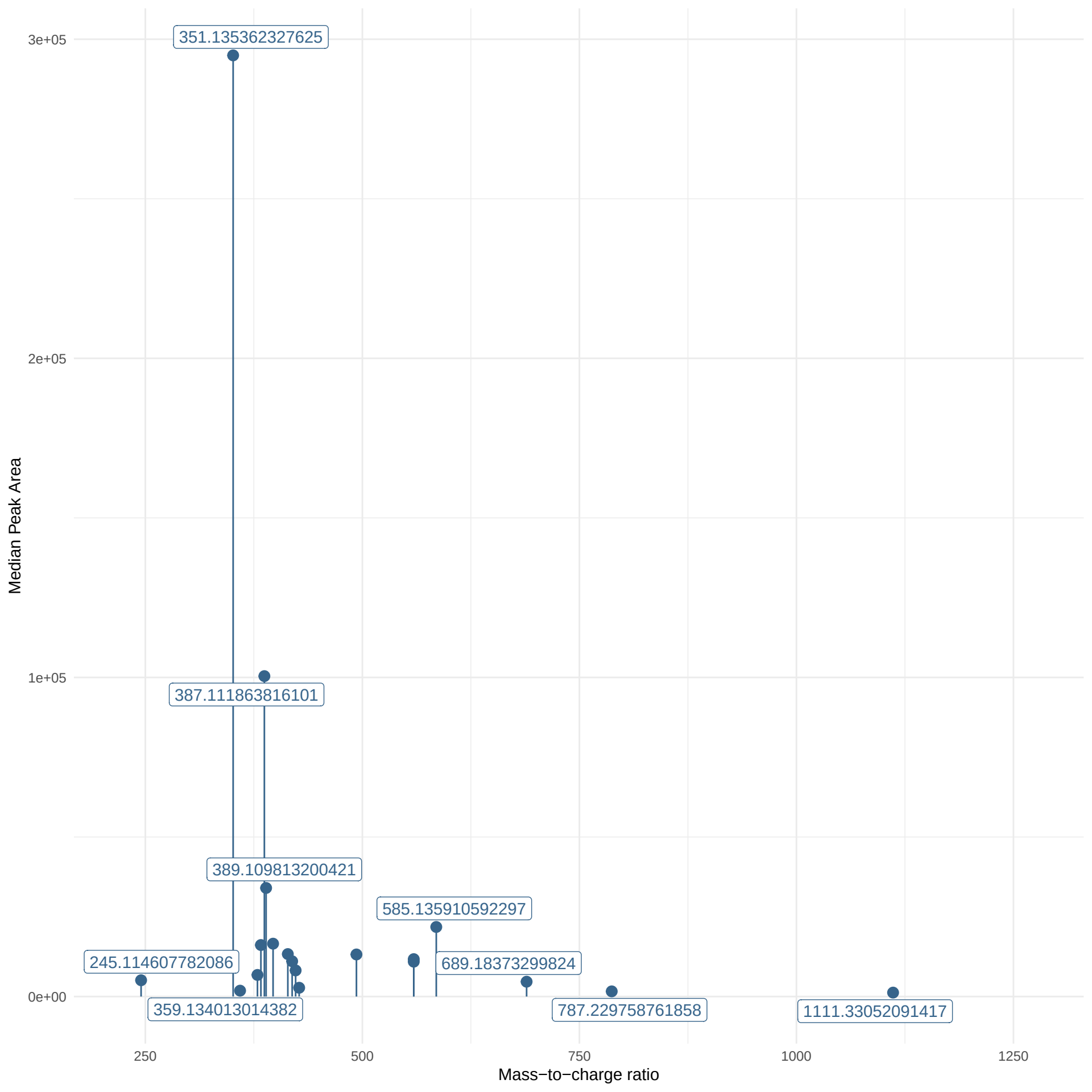
351.135362327625
387.111863816101
389.109813200421
585.135910592297
245.114607782086
689.18373299824
359.134013014382
787.229758761858
1111.33052091417
3e+05
2e+05
1e+05
0e+00
Median Peak Area
250
500
750
1000
1250
Mass−to−charge ratio

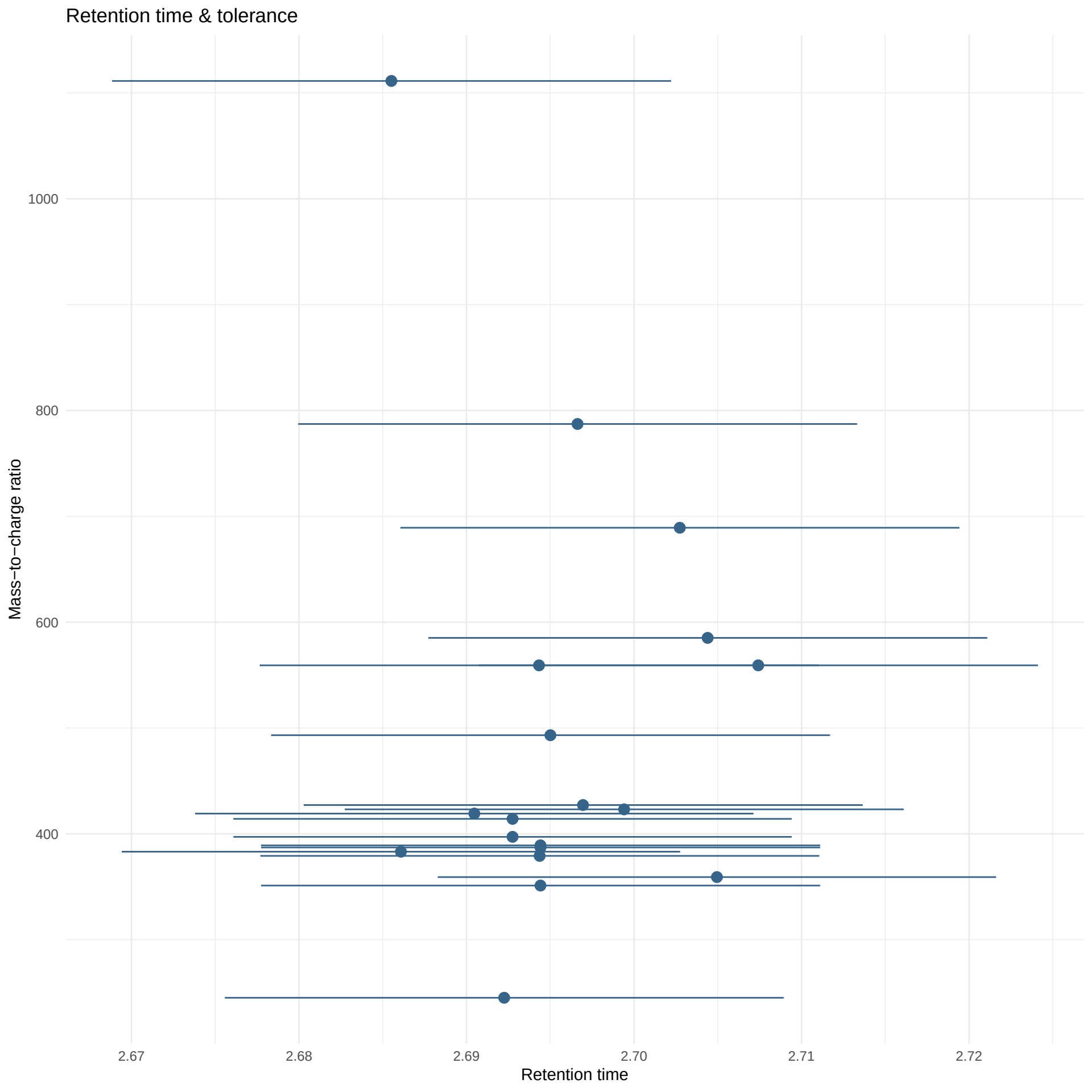
Retention time & tolerance
Mass−to−charge ratio
1000
800
600
400
2.67
2.68
2.69
2.70
2.71
2.72
Retention time

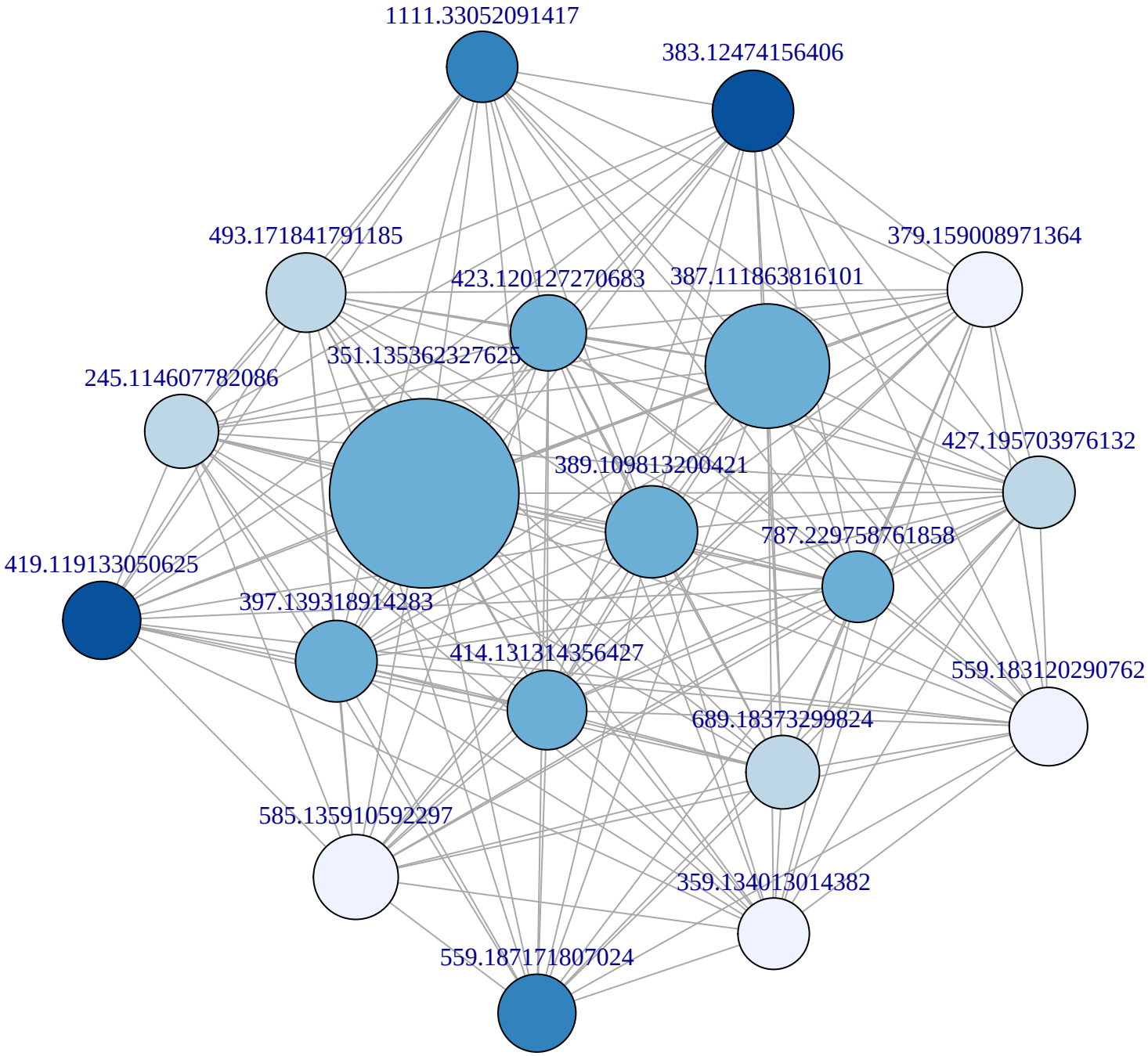
1111.33052091417
383.12474156406
493.171841791185
379.159008971364
423.120127270683
387.111863816101
351.135362327625
245.114607782086
427.195703976132
389.109813200421
787.229758761858
419.119133050625
397.139318914283
414.131314356427
559.183120290762
689.18373299824
585.135910592297
359.134013014382
559.187171807024